The Bioscan
AN INTERNATIONAL QUARTERLY JOURNAL OF LIFE SCIENCES
20(3): S.I (3), 1088-1100, 2025 www.thebioscan.com

Photocatalytic behavior of Pt doped ZnO Nanoparticles in Methylene blue dye degradation

Irine T. M[1*], S. Loice Bessylet[2], Abisha S Santham[3]

[1*]Assistant professor,Loyola Institute of Technology and science, Thovalai,kanyakumariDist, Tamilnadu

[2] Assistant professor,Loyola Loyola Institute of Technology and science, Thovalai, kanyakumariDist, Tamilnadu

[3]Assistant professor, Mar Ephraem College of Engineering and Technology, ElavuvilaikanyakumariDist, Tamilnadu

([1,2,3] Affiliated to Anna University, Chennai)

*Corresponding Author

Email: irinephysics22@gmail.com

DOI: 10.63001/tbs.2025.v20.i03.S.I(3).pp1088-1100

KEYWORDS
Platinum, Combustion, photocatalytic activity, ZnO, nanoparticles, methylene blue
Received on:

20-07-2025

Accepted on:

18-08-2025

Published on:

27-09-2025

ABSTRACT

Preparation of Platinum doped Zinc oxide nanoparticles was carried out using a combustion method at 500 °C. Zinc oxide nanoparticles were doped by different weight percent of platinum (1.0, 3.0, and 5. 0wt %). In this paper, with the aim of increasing its photocatalytic activity, zinc oxide (ZnO) was doped with Platinum (Pt). Characterization of the synthesized powders was done by X-ray diffraction (XRD), Thermogravimetric Analysis, FTIR, UV-Vis spectra, UV-Visible DRS. The prepared samples of photocatalytic performances were studied for degradation of methylene blue dye under UV irradiation. The XRD results showed successful doping of Pt in ZnO. XRD pattern of pt doped ZnO which is only composed the Zincite-type ZnO. It revealed that the size of Pt-doped particles was in the range of 63-82 nm. From TG curve shows 3.0 % sample revealed the best weight loss performance. Fourier transform infrared (FTIR) spectrum indicates the presence of Pt–ZnO stretching vibration at 418cm $^{-1}$ UV-visible absorption peaks at 360 nm, its band gap decreased from 2.78 to 2.14 eV. The photocatalytic activity of platinum doped Zinc oxide nanoparticles was measured under UV irradiation for methylene blue dye degradation. The results showed that the 1% Pt-doped ZnO sample revealed the best performance. The resulting mixtures were irradiated with UV light for a period of 45 mins. The photocatalytic efficiency of 1% Pt- ZnO sample increased from 35% to 75%. Pt doped ZnO nanoparticles show better photocatalytic activity for the degradatiion of methylene blue compared to undoped ZnO nanoparticles.

INTRODUCTION

The industrialization of the 20th era lead to an increase and release of industrial pollutants to the aquatic water system and wastewater [1]. Although numerous procedures have been developed for the treatment of wastewater [2,3]. In recent years, with the fast-developing dye-related industry, an enormous quantity of dye wastewater is nonstop discharged to the water [4]. Which has been a huge danger to the ecological environment and human health. Various dangerous engineered dyes (cationic and anionic) have been invented with high creation rate. To dispose of their negative effects, the wide utilization of composite was watched for oxidative degradation/expulsion of colours from wastewater. In cationic dye, methylene blue, Splendid Blue-R, and Rhodamine-B, while in anionic dye, Methyl orange, Congo red, Alizarin red S and Eosin Y, are generally treated with composite [5]. Methylene blue (MB) is a normally used cationic dye that can form a stable solution with water at room temperature [6,7]. It is damaging to human health above a certain concentration due to its strong toxicity. In addition, almost all dyes are difficult to biodegrade and have some resistance to ecological conditions, making sewage treatment a vital project [8,9]. Therefore, it is mostly important to change effective and low-cost materials to eradicate MB and other dyes from wastewater and refresh the environment

Dyes are broadly used as colouring agents in the textiles, leather, food, plastics, cosmetics, and other industries [10,11]. However, greatest industrial dyes are toxic, carcinogenic, and mutagenic, and have low biodegradability [12]. Moreover, dye-containing effluents are highly coloured, so removal of these effluents into natural water bodies affects the balance of aquatic environments because they can stop the penetration of sunlight into the water, which results in a reduction in dissolved oxygen content [13]. Therefore, the elimination of dyes prior to the discharge of wastewater from dye industries is of great importance. Most current physicochemical and biological treatment methods, which contain carbon adsorption, flocculation, ozonization, and activated sludge processes, fail to totally destroy dye pollutants, and are also slow, require expensive equipment, and can lead to secondary pollution [14-16].

Various important industries, such as textile and leather, depend fundamentally on dyes owing to its colour-giving properties. It is

assessed that thousands tones of commercial dyes are produced [17–20]. One of the greatest attractive industries that use dyes is textile industry that may consume over than 10 thousand tons of dyes universal per year [21]. It has been determined that the dye wastewater from textile industry is created as a result of the difficulty of whole attachment of the dye mixture onto a piece of fabric or textile [22]. Many dangerous chemicals such as organic resins, organic solvents hydrogen peroxide, formic acid, dispersing agents, soap, caustic soda, sulphuric acid, and hydrosulphate are included in dye wastewater. All these chemicals are known by its hazard and toxic effects towards are lives of humans and animals owing to their toxic nature [23,24]. Newly, elimination of dye molecules from wastewater is a vital issue and has a wide environmental anxiety [25]. Varied techniques of dye removal from wastewater have been discovered, but not all of them are effective and fruitful owing to their disadvantages [26,27]. In fact, two important issues are governing the efficacy of the dye removal method namely; time is taken for the removal method to be completed and production of secondary pollutants. Obviously, the removal method to be efficient in dye removal from dye wastewater it should remove large quantities of dyes in short time without yielding more secondary hazardous products. Researchers have involved three categories of dye removal procedures from wastewater namely (i) biological method: this method is characterized by its low cost and ease of performance whereas; it is unable to remove dyes effectively from wastewater [28]. (ii) chemical method: this method uses chemistry and its theories to be proficient; several mechanisms may be involved in chemical methods such as electrochemical, advanced oxidation processes (AOPs), reduction, ozonation, and Fenton reaction; this method is characterized by the high cost beside generation of secondary hazardous by-products [29]. (iii) Physical method: this method is commonly achieved through mass transfer mechanism; physical method may be performed through many strategies such as flocculation, reverse osmosis, adsorption, ion exchange, irradiation, membrane filtration, coagulation and ultrafiltration [30-32]. Chemical dye removal is the most effective method among all mentioned approaches although of its disadvantages.

Various methods, including ultrafiltration [33], reverse osmosis [34], adsorption on numerous materials such as initiated carbon [35], wood chips [36], and silica gel [37] have been conveyed to remove toxins from industrial wastewaters. One of the important drawbacks of the methods revealed is the change of the aqueous phase into a stable network (secondary pollution) and the use of numerous steps for purification, which is costly and time-consuming [38]. Metallic elements growth the time required for electrons to return to the valence band due to the generation of additional bands near the conduction band (trap bands). The longer existence of electrons in the conduction band increases the possibility of their reacting with the peripheral ions and thus enhancing photocatalytic activity [39,40].

In recent years, photocatalytic materials have established much attention due to minor side effects and hardly any secondary pollution after wastewater treatment and pollutant removal [41,42]. Metal oxides such as ZnO, TiO2, Fe2O3, Cu2O, WO3, have been of interest to researchers for their photocatalytic applications [43-47]. Among the photocatalytic materials, n-type semiconductors, such as ZnO, are the maximum prominent. Due to the reality of a free electron in the ZnO semiconductor, the number of holes created in the valence band is less than that of electrons created in the conduction band [48]. ZnO has not been thoroughly studied as catalyst [49]. A semiconductor appropriate for photocatalysis has to be (i) photoactive, (ii) able to use visible or near-UV light, (iii) biologically and chemically inert, (iv) photo-stable, and (v) of reasonably low cost [50]. In semiconductors, zinc oxide (ZnO) is the one that fulfills all the previous conditions. In nanostructure forms, both of these oxide semiconductors (TiO_2 and ZnO) should work as better catalysts/photocatalysts due to their high precise surface areas [51]. Usually, the properties of nanomaterials be determined on their size, morphology, and dimensionality. Semiconductor nanostructure catalysts have been used traditionally not only to produce useful chemicals [52], but also to convert pollutants in waste streams to inoffensive or less harmful form [53–55]. Heterogeneous photocatalysis is an advanced oxidation process (AOP), which produces hydroxyl radicals (•OH) by oxidation of adsorbed OH− or H_2O molecules on a semiconductor surface while it is irradiated with light of energy greater than its band gap [56]. The •OH radicals are enormously powerful oxidants, being able to degrade a great variety of organic compounds [57]. The high surface reactivity of ZnO results in the development of many defects derived from non-stoichiometric oxygen, which makes ZnO a more effective photocatalyst in comparison to other metal oxides [58-60]. Doping is one of the methods to change the band structure and band gap of ZnO [61]. To raise the photocatalytic efficiency of ZnO, i.e., reduction of the bandgap and recombination rate, doping elements such as Co [62], Mn [63], Fe [64], Cr [65], Cu [66], Al [67], Sn [68], as well as noble metals such as Pd [69], Pt [70], and Ag [71] have been studied. Platinum-based catalysts have revealed high activity for many reactions, but noble metal platinum has a main problem in its limited availability. It is always attractive to decrease the usage of platinum while keeping significant catalytic performance. Thus, using a small amount of platinum to modify other nonnoble active sites offers an alternative approach, and many exciting results have been reported [72−74]. At the nanoscale, Pt Nps have also been engineered, primarily for catalytic application [75]. Nowadays, it is believed that surface states can be greatly improved by catalytic noble metals, such as Pt [76-79]. In this study, the photodegradation of MB using ZnO doped with platinum was investigated. The reaction conditions and the optimum percentage of Pt used in doping the ZnO particles were also investigated.

2. EXPERIMENTAL PROCEDURE

2.1 MATERIALS

Zinc Nitrate ($Zn(NO_3)_2\ 6H_2O$), Glycine ($C_2H_5NO_2$), Citric acid ($C_6\ H_8\ O_7$), Platinum tetrachloride ($PtCl_4$), methylene blue ($C_{16}\ H_{18}\ ClN_3\ SxH_2O$) and Distilled water was used all over the experiment.

2.2. PREPARATION OF ZNO NANOPARTICLES

Preparation of ZnONps by combustion method zinc nitrate ($Zn(NO_3)_2{\cdot}6H_2O$), used as oxidizer, Glycine $C_2H_5NO_2$) and Citric acid ($C_6\ H_8\ O_7$) as fuel. Stochiometric ratio 1:4 of zinc nitrate acted as oxidant and fuel (Glycine, Citric acid) are taken with 30 ml of water in the 100 mL beaker and stirrer to form is homogeneous mixture. The mixture solution is transferred to 1000 ml beaker and kept hot plate and the solution was boiled. After few minutes the solution was changed to foam and the water molecules evaporated. After the mixture solution changed like bubbles with pale yellow colour. Combustion occurred instantaneously leading to explosion After few minutes burned and it turned ash. These combustion taking place within 5-15min, reaction proceeds and finally form a nanoparticles of ZnO. The products were calcined at 500 $^{\circ}C$ for 4 hour.

2.3.SYNTHESIS OF PLATINUM DOPED ZINC OXIDE NANOPARTICLES

Pd-doped ZnOnanopowders were synthesized by combustion method using zinc nitrate ($Zn(NO_3)_2{\cdot}6H_2O$), glycine ($C_2H_5NO_2$) and Citric acid ($C_6\ H_8\ O_7$) as starting materials and (Platinum tetrachloride ($PtCl_4$) as doping source. Zinc nitrate and palladium acted as oxidant while glycine and citric acid as fuel during the reaction. The fuel to oxidant molar ratio was adjusted to 1:4 as it exhibited enhanced photocatalytic activity. To zinc nitrate solution with Platinum tetrachloride (1.0 wt.%, 3.0 wt.%, and 5.0 wt.%), glycine and citric acid solution taken with 30 ml of water in the 100 mL beaker and strirrer to form is homogeneous mixture. The mixture solution is transferred to 1000 ml beaker and kept hot plate. Under boiling, with evaporation of water, the solution turned viscous generating small bubbles with brownish colour. Combustion occurred instantaneously leading to explosion. In the combustion reaction, large amount of heat and non-toxic gases explosively evolved, resulting in dry, loose and voluminous nanocrystalline powders with high porosity. It was observed that the as-synthesized nano powders were of brownish colour. These combustion taking place within 5-15min, reaction proceeds and finally form a nanoparticles of ZnO. The products were calcined at 500 $^{\circ}C$ for 4 hours. The prepared Pt-doped ZnO samples with molar concentration of 1.0 wt.%, 3.0 wt.%, and 5.0 wt.% as shown in fig.1.

2.4. PHOTOCATALYTIC EXPERIMENT

0.001 M methylene blue stock solution was prepared by taking 0.032 g of methylene blue in 100 ml distilled water. For the photocatalytic degradation methylene blue was taken as the sample as it has been extensively used as an indicator for the photocatalytic activites, 0.1 g of platinum doped and undoped photocatalyst was added to 50 mL of 10 μM methylene blue solution and kept in dark condition. The solutions were subjected to irradiation of UV lamp (Philips TUV 15 W/G15 T8(UV-C,λmax=253.7nm)) under continuous stirring. The experiment was continued for 45 minutes to aquire the equilibrium of adsorption – desorption in dispersed solutions and were irradiated of radiation and in regular time interval 0.5 ml sample was collected and absorbance was measured .The solution was taken every 5 minutes and centrifuged and the sample was analyzed by double beam UV Visible spectrophotometer and the absorbance was measured at 661nm. The percentage of degradation can be calculated using the formula [80] which shows eqn (1)

$$\% \text{ of degradation} = \frac{C_i - C_f}{C_i} \times 100 \text{ ----------(1)}$$

Where $C_i$represents for the absorbance value of first peak, C_f represents for changed the absorbance value of other peaks.

Fig.1. Platinum doped Zinc oxide Nps for different weight percentage

3. Results and Discussion

3.1 XRD Studies

The X-ray diffraction pattern of pure and Pt-doped ZnO samples shown in fig.2. The Rietveld refinement was done using BRUKER TOPAS v6. The following parameters were initially refined, i) Background was fitted using a Chebychev Polynomial of order 5, ii) peak shape was modelled using Fundamental Parameter (FP) approach. The peak positions confirm the hexagonal Zincite structure of synthesised samples (JCPDS card no. 65-3411). The overall intensity of the XRD peaks increased with the use of platinum doping different percentage weight of ZnO annealing the sample with 500^{o}C degree, based on the XRD patterns, the lattice parameters and crystallite sizes as function of the platinum doped with ZnO process are calculated in Table.1 A small variation of the lattice parameters and cell volume was observed. The peaks of pure and Pd doped ZnO are obtained at (100), (002), (101), (102), (110), (103), (200), (112), (201), (004) and (202) planes. No peaks corresponding to Pt metal or platinum oxide are present which implies that dopant is successfully doped in ZnO lattice. These results suggest that zinc oxide's phase structure remained unchanged during platinum deposition and remained pure [81] The crystallite size calculated using Scherrer's formula in eqn .2

$$D = \frac{k\lambda}{\beta \cos\theta} \text{ ---------- (2)}$$

D is the crystallite size, λ is the wavelength (1.54 Å), of the x-ray source, β is the full width at half maximum, θ is the Braggs diffracting angle. K is Scherrer constant (0.9 Å).

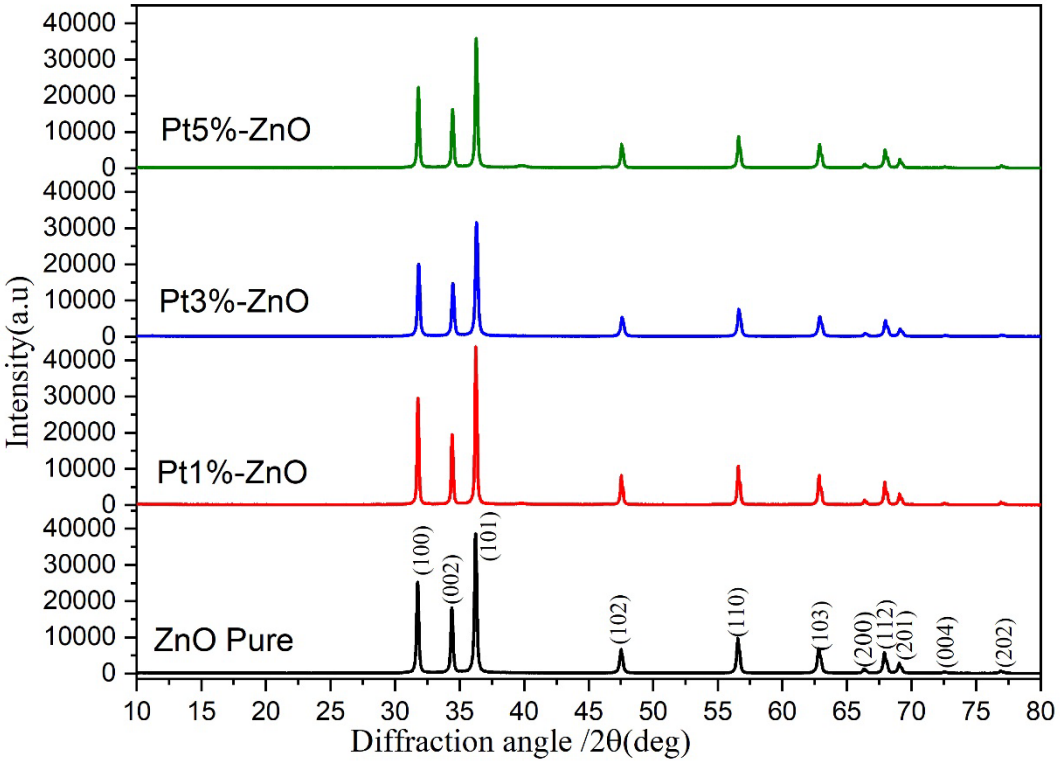

Fig. 2 XRD Patterens of ZnO Pure and Pt doped ZnO

Table. 1.Geometric and lattice parameters for ZnO and Pt-doped ZnO nanoparticles as determined by XRD

sample	Lattice parameters (Å)		a-c Volume (Å3)	Crystallite size (D) (nm)
	a = b	c		
ZnO Pure	3.25159	5.21109	47.12	47
ZnO – Pt 1%	3.24848	5.20818	47.59	82
ZnO – Pt 3%	3.2524	5.2109	47.73	67
ZnO – Pt 5%	3.2526	5.2092	47.72	75

3.2. Thermogravimetric Analysis

The absorbed water content was determined from the weight difference measured at 0ºC -800º C from thermogravimetric data. From Fig. 3, TGA curves shows ZnOnanoparticles doped platinum. It shows a continuous weight loss on heating. The observed weight loss is due to removal of water from the samples. In ZnO pure sample fig 4.a, the first thermal decomposition stage takes place at room temperature around 100 ˚C, which can be observed as a weight loss of 7% in thermogravimetry curve attributed to the removal of adsorbed water, in the next stage leading the thermal decomposition, ranging from 200º C to 500º C a weight loss of 15 % was observed in ZnO. The net weight loss 22 % was observed beyond 700 º C in ZnO, From fig 4.b shows platinum doped 1.0 wt % level of ZnO the first thermal decomposition stage takes place at room temperature around 75 ˚C, which can be observed as a weight loss of 5%, in the next stage leading the thermal decomposition, ranging from 100º C to 450º C a weight loss of 8 %, The net weight loss 13 % was observed beyond 550 º C was observed, From fig 4.c shows platinum doped 3.0 wt % level of ZnO the first thermal decomposition stage takes place at room temperature around 50 ˚C, which can be observed as a weight loss of 3%, in the next stage leading the thermal decomposition, ranging from 75º C to 400º C a weight loss of 5 %, The net weight loss 8 % was observed beyond 450 º C was observed, From fig 4.d shows platinum doped 5.0 wt % level of ZnO the first thermal decomposition stage takes place at room temperature around 70 ˚C, which can be observed as a weight loss of 4%, in the next stage leading the thermal decomposition, ranging from 100º C to 450º C a weight loss of 6 %, The net weight loss 10% was observed beyond 500 º C was observed a thermal decomposition stage related to the total combustion of organic waste and consequent crystallization of the crystalline phases.

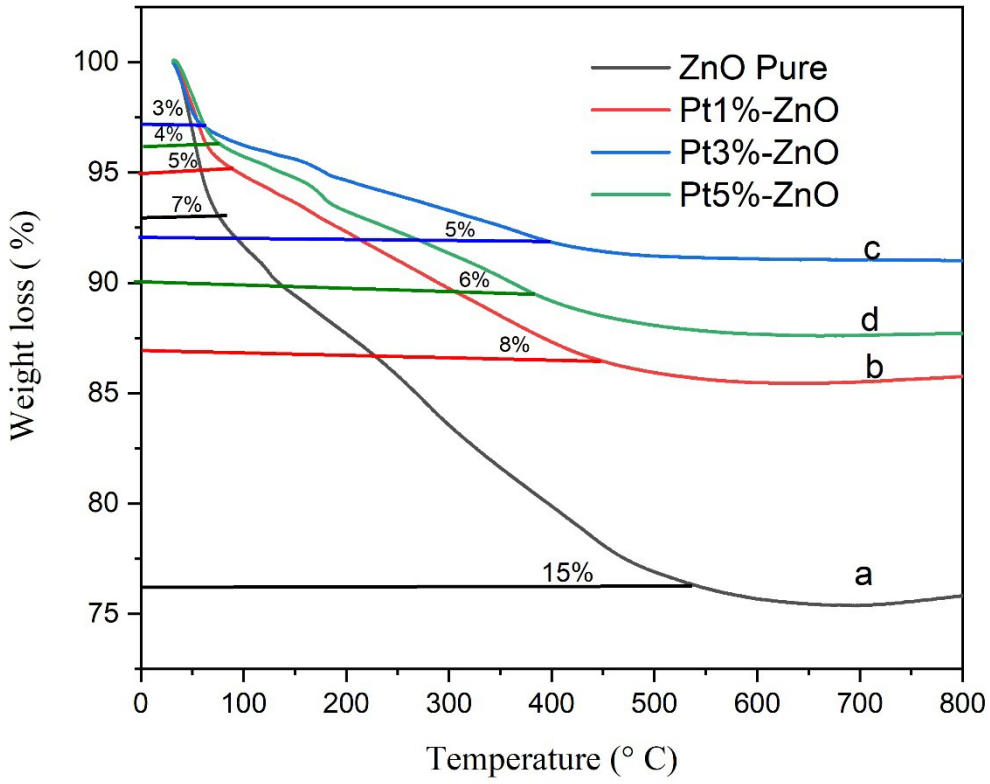

Fig.3 Thermogravimetric Analysis of ZnO Pure and Pt doped ZnO

3.3 UV-Visible absorption Analysis

UV-Vis spectroscopy analyses were achieved to determine the effect of Pt amount on the optical properties of the ZnO nanoparticles. Figure 4 shows the UV-Vis spectra of the ZnO and Pt doped ZnO nanoparticles. Pure ZnO and Pt doped with different percentage level to the ZnO nanoparticles all the spectra revealed sharp absorption edge at about 360 nm, characteristic of crystalline ZnO. It has been shown that the particle size of nanoparticles affects their optical properties [82]

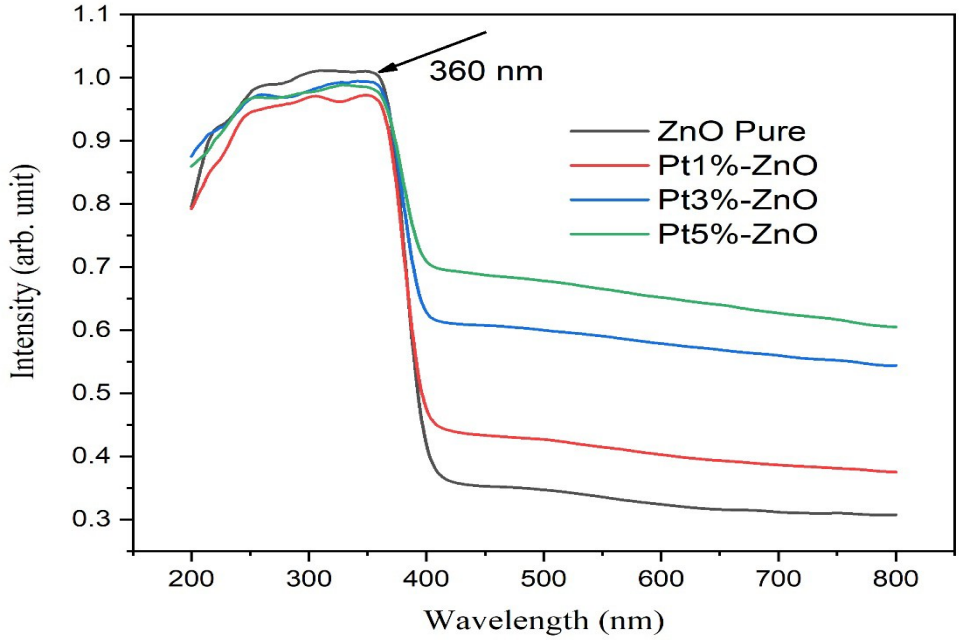

Fig.4 UV-Visible spectrum of ZnO Pure and Pt doped ZnO

3.4 Band gap determination

The optical band-gap of the ZnO pure and Pt doped ZnO nano particles can be determined with a well-known Tauc's model by using Mott and Davis relation $\alpha h\upsilon \sim (h\upsilon - Eg)^{\frac{1}{2}}$ where Eg is energy band gap. Following this relation, the band gap is attained by extrapolating the tangential line of $(\alpha\, h\upsilon)^2$ to the photon energy axis. The direct bandgap energies can be estimated from a plot of $(\alpha\, h\upsilon)^2$ versus the energy (Eg) are obtained by by plotting the absorption coefficient (a)-photon energy graph (hu) and extrapolating the straight-line portion of this plot to the hu axis as shown in the Fig. 5. For the pure ZnO nanoparticles Eg was determined as 2.782 eV, which decreases to 2.561, 2.358, 2.148 eV respectively for the different percent Pt doped ZnO nanoparticles. The band gap energy of all nanostructures was calculated dependent on the absorption spectrum of the sample according to the following Eq. (3):

$$Eg = 1240/\lambda_g \quad \text{---------- (3)}$$

Where, Eg is the optical band gap energy of the photocatalyst, λ_g is the wavelength in nm used as the absorption edge. Also the band gap energy was determined using Tauc's formula which shows the relationship among absorption coefficient as follows (Eq. (4)):

$$\alpha\, h\upsilon)^2 = B\,(\, h\upsilon - Eg\,) \quad \text{---------- (4)}$$

Where a is the absorption coefficient, h is Planck's constant and υ is the frequency (υ = c/$\boldsymbol{\lambda}$, $\boldsymbol{\lambda}$ is wavelength, c is light speed) [83]. B is a constant called band tailing parameter. Thus, the band gap energy was obtained graphically from $(ah\upsilon)^2$ vs hυ for direct transition, extrapolating the linear part according to Eq. (4) in (Fig. 6). there is no significant influence of the doped platinum on the band gap energy (Eg) value of the ZnO nanoparticles

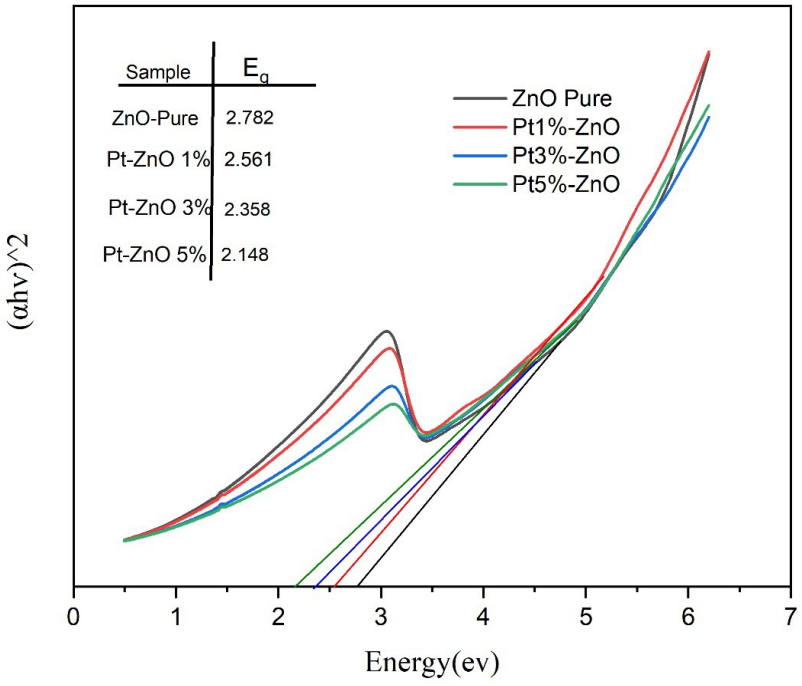

Fig.5 Band gap spectrum of ZnO and Pt doped ZnO

3.5 Diffuse- reflectance spectrum Analysis

The diffuse-reflectance spectra of ZnO and Pt doped ZnO nanoparticles are shown in Fig 6. It revealed characteristic absorption edge near 370 nm. The ZnO nanoparticles exposed high reflectance in the visible region comparing the Reflectance of the all samples of Pt-doped ZnO samples. Reflectance of the Pt-doped ZnO samples decreased. The reflectance at wavelengths bigger than 370 nm can be related to the direct bandgap of ZnO and Pt doped ZnO due to the transition of an electron from the valence band to the conduction band. While absorption edge did not change noticeably, the reflectance value decreased with the increase of Pt content in the composite samples.[84]

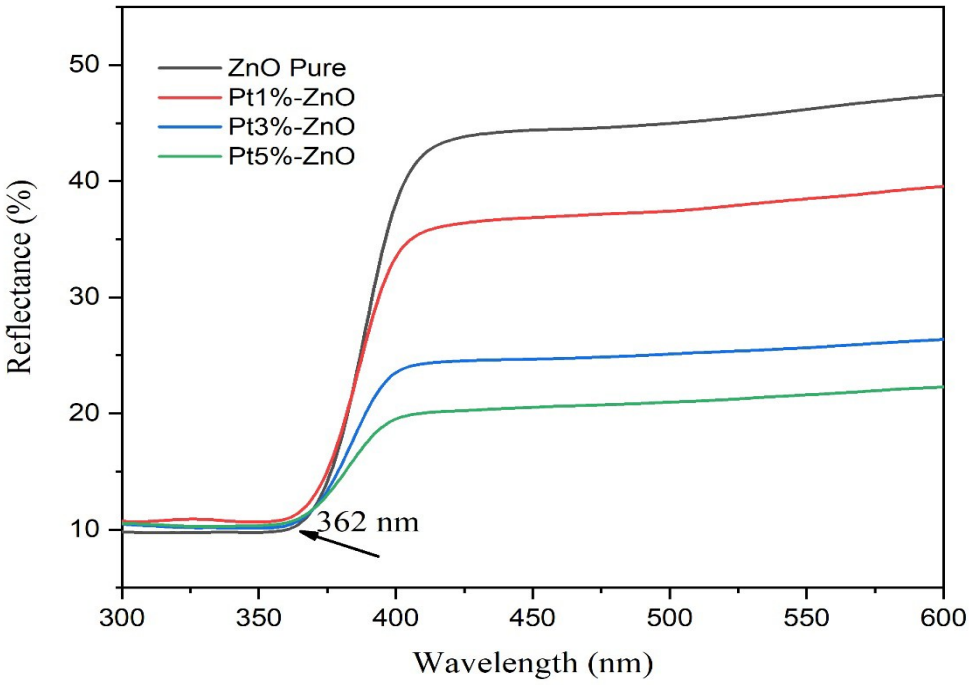

Fig.6 UV-Diffuse Reflectance spectrum of ZnO and Pt doped ZnO

3.6. FTIR Analysis

FT-IR spectra for ZnO and Pt doped nanoparticles in the range of 400-4000 cm^{-1} were recorded and the results can be seen in Fig. 8. The broad transmission band at 418 cm^{-1} (which is indicated by arrow) was assigned to stretching vibration of Zn-O bond which the formation of zinc oxide [85],which is shown in Fig.7. whereas the bands at 3200-3600 cm^{-1} correspond to O-H mode of vibration. The FTIR characteristic peaks of the spectrum is given in the table.2

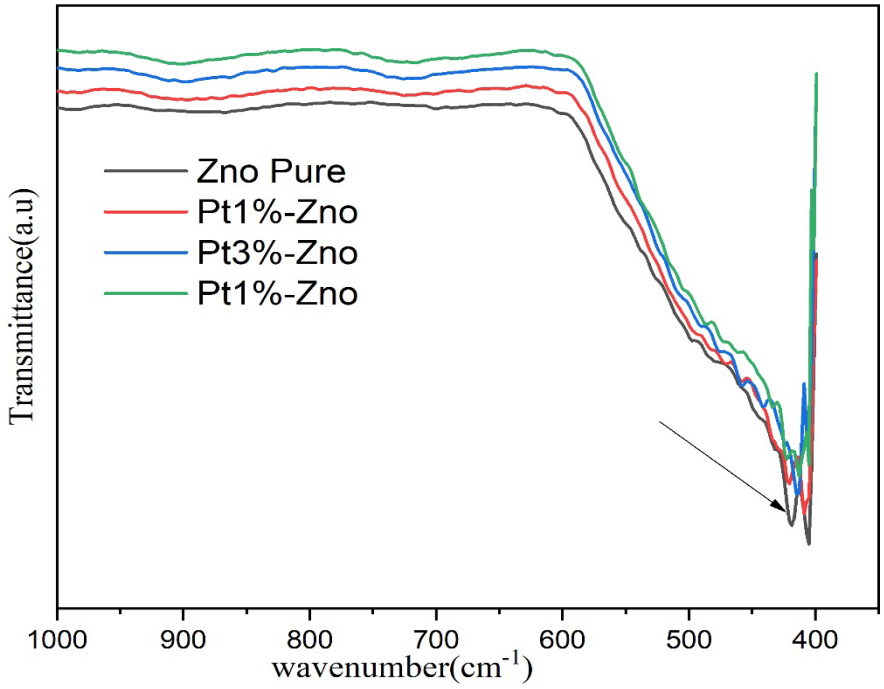

Fig. 7 FTIR enlarged portion of the spectra from 400 cm^{-1} to 1000 cm^{-1} of ZnO and Pd doped ZnO nanoparticles.

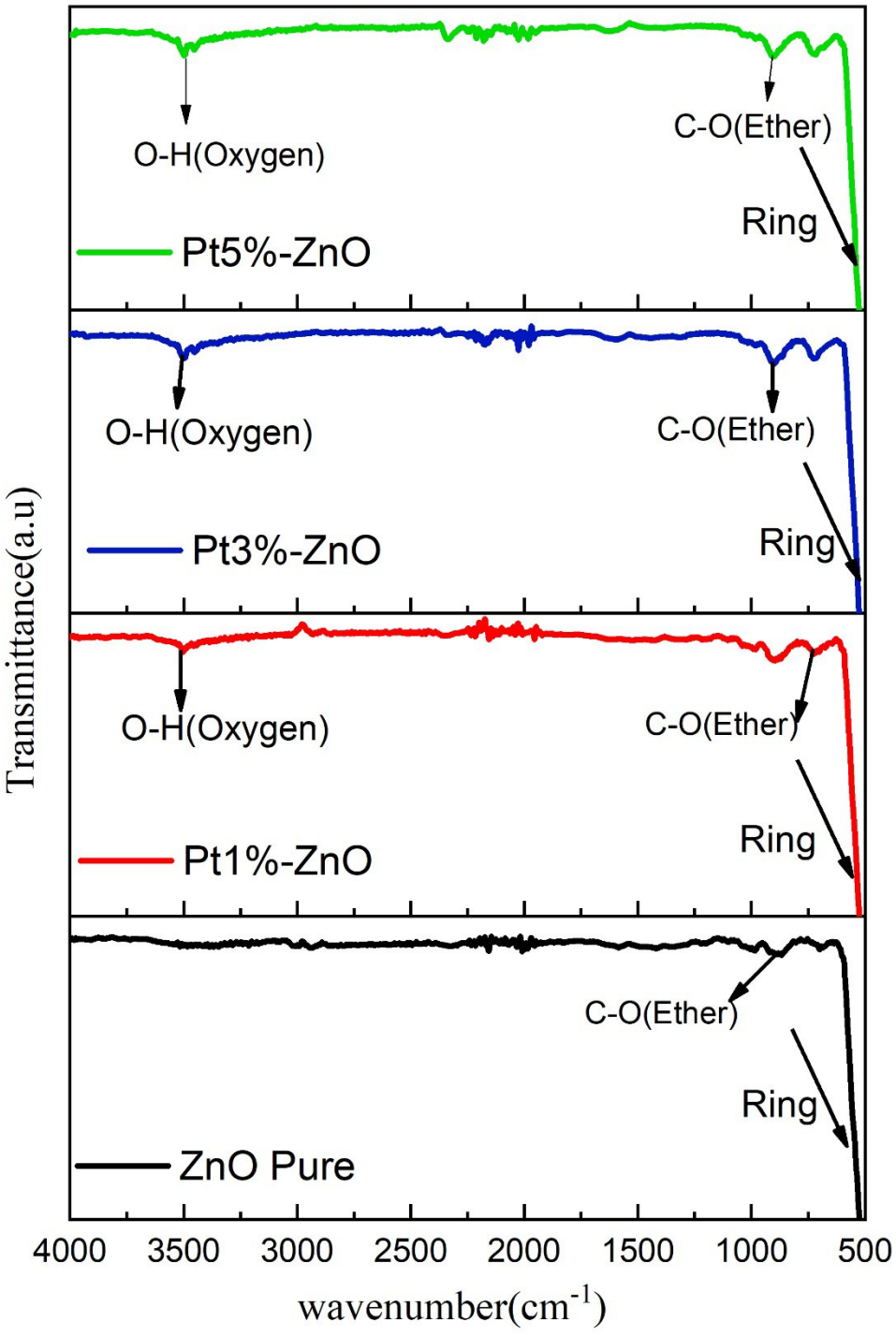

Fig. 8 FTIR Spectrum of ZnO and Pt doped ZnO nanoparticles

Table 2: Characteristic peaks in FTIR spectrum of Pt doped ZnO

Samples	Peak values Frequency cm^{-1}	Bond	Functional groups
ZnO Pure	418.55	Ring	Meta
	879.54	C- O	Ether
	983.70	C- O	Ether
Pt 1%-Zno	420.48	Ring	Meta
	459.06	Ring	Meta

	717.52	C-O	Ether
	896.90	C-O	Ether
	3502.73	O-H	Oxygen group
Pt 3%-Zno	414.70	Ring	Meta
	725.23	C-O	Ether
	898.83	C- O	Ether
	3495.01	O-H	Oxygen groups
Pt 5%-Zno	420.48	Ring	Meta
	486.06	Ring	Meta
	727.16	C-O	Ether
	900.76	C- O	Ether
	3498.87	O-H	Oxygen groups

3.7 Photocatalytic study

The photocatalytic activities of the samples were evaluated by the photocatalytic degradation of methylene blue (MB) dye under UV irradiation. The UV–vis absorption spectra of MB at different irradiating intervals using the ZnO powders and platinum doped ZnO synthesized as 500° C Calcination of photocatalysts. From fig.9(a-d) As can be seen, the intensities of the absorption peak situated at 661 nm decrease with the increase of the irradiation time, indicating that the concentration of MB in the solution is reduced gradually. the absorbance vs wavelength plots with respect to time showing dye degradation using ZnO Pure, Pt 1.0 wt % -ZnO, Pt 3.0 wt% -ZnO, Pt 5.0 wt% -ZnO samples within time 45 minutes[86]. As seen in the figures, it is observed that the peak intensity of the absorption was decreased when the time is increased for all the Pt-ZnO NPs. The absorption intensity was almost disappeared at 45 min irradiation time of UV light, From fig.9. b The maximum degradation of methylene blue dye degradation was achieved using Pt 1%-ZnO comparing other samples. This made Pt 1%-ZnO to be fast and highly photocatalytic activity

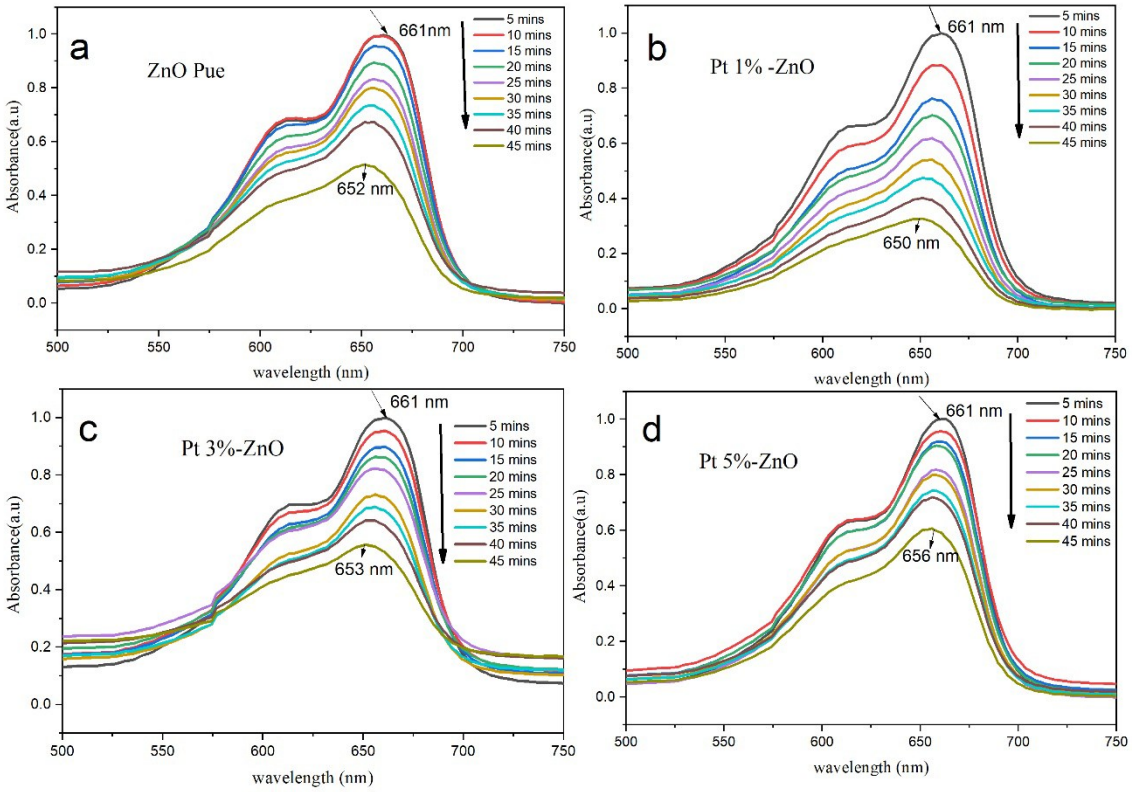

Fig.9. Photocatalytic spectrum of Pt doped ZnO

3.8 Degradation Efficiency

Figure .10 shows the photodegradation efficiency (%) for 45 minutes irradiation time for ZnO and different weight percentage of Pt doped ZnO samples of 1.0 wt %, 3.0 wt %, 5.0 wt %. The photodegradation efficiency was found to be, 60%, 75%, 40%, 35% for ZnO, 1.0 wt %, 3.0 wt %, 5.0 wt % respectively (87) The 1.0 wt % of Pt doped ZnO sample showed the highest photocatalytic behavior when compared to other samples. Increasing the catalyst concentration for 3.0 wt % and 5.0 wt %, decreases the degradation efficiency. it clearly demonstrated that ZnO doped with low concentration of Pt degrades dye more efficiently than pure ZnO. It is evident that doping of ZnO with noble metals like Pt enhances photocatalytic activities of ZnO. This provided a Combustion method to synthesize zinc oxide with excellent photodegradation property for methylene blue Consequently, decreased the surface area of photocatalyst and decelerates the oxidation and reduction process of MB solution. The photocatalytic activity of the composite catalysts was further enhanced in Pt doped ZnO. Amongst these composites, the 1% Pt doped ZnO nanocomposite catalyst had the maximum degradation efficiency for the MB dye. Further increase in platinum doping concentration not improving the dye degradation.

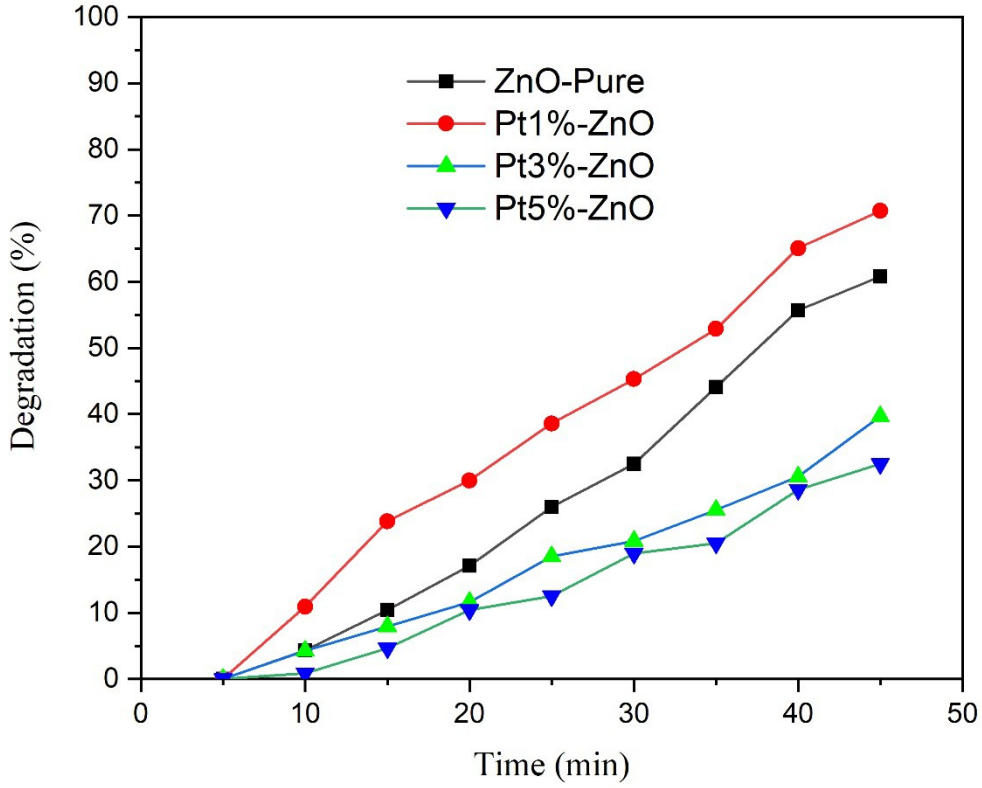

CONCLUSION

Doping different molar percentages of Pt in ZnO nanoparticles was performed by the combustion method. and characterized by TG, UV-DRS, XRD, FTIR. The results of phase analysis showed that the Pt element entered the ZnO lattice, and with increasing Pt doping percentage, the crystallite size and lattice parameter were changed. The results showed that synthesized zinc oxide and Platinum doped zinc oxide nanoparticles exhibited UV-visible absorption peaks at 360 nm, and doped Platinum Zinc oxide was decreased bandgap energy from 2.782 eV, 2.561, 2.358, 2.148 eV. The UV-DRS displayed the optical properties and FTIR shows a band at 418 cm $^{-1}$ and 459 cm $^{-1}$ due to Zn–O and Pt–ZnO vibrational stretching. The results of the dye degradation showed that the sample containing 1% Pt was the sample for photocatalytic activities. MB dye degradation test results showed that 1% Pt had a much higher performance in comparison to another sample; 35-75%. at 45 min, which improve more 40% than that of another sample, the improvement of photocatalytic activity contributes to the increased adsorption ability of light.

REFERENCES

- Abdullah Iqbal, M, Ali, SI, Amin, F, Tariq, A, Iqbal, MZ &Rizwa, S, 2019, 'La- and Mn-Codoped Bismuth Ferrite/Ti_3C_2MXene Composites for Efficient Photocatalytic Degradation of Congo Red Dye', ACS Omega, Vol.4, no.5, pp. 8661−8668.
- Gupta, VK, Agarwal, S & Saleh, TA, 2011, 'Synthesis and characterization of alumina-coated carbon nanotubes and their application for lead removal', Journal Hazardous Materials, Vol.185, no.1, pp. 17−23.
- Rafatullah, M, Sulaiman, O, Hashim, R & Ahmad, A, 2010, 'Adsorption of methylene blue on low-cost adsorbents: a review', Journal Hazardous Materials, Vol. 177, no.1-3, pp. 70−80.
- 4.Pattnaik, P, Dangayach, GS, 2019, 'Analysis of influencing factors on sustainability of textile wastewater: a structural equation approach', Water, Air & Soil Pollution, Vol. 230, no.7, pp. 156.
- Doulati, AF, Badii, K, Yousefi Limaee N, Mahmoodi, NM, Arami M, Shafaei, SZ, 2007, Numerical modelling and laboratory studies on the removal of Direct Red 23 and Direct Red 80 dyes from textile effluents using orange peel, a low-cost adsorbent', Dyes and Pigments, Vol. 73, no.2, pp. 178-185.
- Deng, C, Liu, J, Zhou, W, Zhang, YK, Du, KF & Zhao, ZM, 2012, 'Fabrication of spherical cellulose/carbon tubes hybrid adsorbent anchored with welan gum polysaccharide and its potential in adsorbing MB', Chemical Engineering, Vol. 200−202, pp. 452−458.
- Russo, V, Masiello, D, Trifuoggi, M, Di Serio, M & Tesser, R, 2016, 'Design of an adsorption column for methylene blue abatement over silica: From batch to continuous modeling', Chemical Engineering, Vol. 302, pp. 287−295.
- He, X, Male, KB, Nesterenko, PN, Brabazon, D, Paull, B & Luong, JH, 2013, 'Adsorption and Desorption of Methylene Blue on Porous Carbon Monoliths and Nanocrystalline Cellulose', ACS Applied Material Interfaces, Vol. 5, no. 17, pp. 8796−8804.
- Liu, Y, Wang, J, Zheng, Y, Wang, A, 2012, 'Adsorption of methylene blue by kapok fiber treated by sodium chlorite optimized with response surface methodology', Chemical Engineering, Vol. 184, no. 1, pp. 248−255.
- Martínez-Huitle, CA, & Brillas, E, 2009,Decontamination of wastewaters containing synthetic organic dyes by electrochemical methods: A general review', Applied Catalysis, Vol. 87, no. 1-3, pp. 105–145.
- Xie, Y, Chen, F, He, Zhao, J & Wang, H, 2000, 'Photoassisted degradation of dyes in the presence of Fe^{3+} and H_2O_2 under visible irradiation', Photochemical Photobiolgy A-Chemistry Vol. 136, no. 3, pp. 235–240.
- Gupta, VK, Pathania, D, Agarwal, D & Sharma, S, 2012, 'De-coloration of hazardous dye from water system using chemically modified Ficus carica adsorbent', Molecular Liquids, Vol.174, no.1, pp. 86–94.

- Chen, KC, Wu, JY, Liou, DJ & Hwang, CJ, 2003,'Decolorization of the textile dyes by newly isolated bacterial strains',Biotechnology, Vol.101, no. 1, pp. 57–68.
- Patil, SS &Shinde,VM, 2008,'Biodegradation studies of aniline and nitrobenzene in aniline plant wastewater by gas chromatography',Environmental Science Technology, Vol. 22, no. 10, pp. 1160–1165.
- Vautier, M, Guillard, C, & Herrmann, JM, 2001, 'Photocatalytic Degradation of Dyes in Water: Case Study of Indigo and of Indigo Carmine. Journal of Catalysis', Vol.201, no. 1, pp. 46–59
- Michael A. Anderson, 2000, 'Removal of MTBE and Other Organic Contaminants from Water by Sorption to High Silica Zeolites', Environmental Science & Technology, Vol. 34, no. 4, pp. 725-727
- J. Abdi, M, Vossoughi, NM, Mahmoodi, I &Alemzadeh, 2017, 'Synthesis of metal-organic framework hybrid nanocomposites based on GO and CNT with high adsorption capacity for dye removal', Chemical Engineering, Vol. 326, pp. 1145–1158.
- Crini, G, 2006, 'Non-conventional low-cost adsorbents for dye removal: a review', Bioresource Technology, Vol. 97 no. 9, pp. 1061–1085.
- Gupta, VK & Suhas, 2009, 'Application of low-cost adsorbents for dye removal–a review', Environmental Management, Vol. 90, no. 8, pp. 2313–2342.
- Holkar, CR, Jadhav, AJ, Pinjari, DV, Mahamuni, NM & Pandit, AB, 2016, ' A critical review on textile wastewater treatments: possible approaches, Environmental Management, Vol.182, pp. 351–366.
- Rodríguez-Couto, S, Osma, JF & Toca-Herrera, JL, 2009, 'Removal of synthetic dyes by an eco-friendly strategy', Engineering Life Science, Vol. 9, no.2, pp. 116–123.
- Robinson, T, McMullan, G, Marchant, R & Nigam, P, 2001, 'Remediation of dyes in textile effluent: a critical review on current treatment technologies with a proposed alternative', bioresource technology Vol. 77, no. 3, pp.247-255.
- M.A.M. Alwani, AL, Norasikin, AL, Mohamad, A, A.H. Kadhum, A, Mukhlus, A, 2018,'Application of dyes extracted from Alternanthera dentata leaves and Musa acuminata bracts as natural sensitizers for dye-sensitized solar cells, Spectrochim Acta A Mol BiomolSpectrosc. Vol.192, pp. 487–498.
- Liu, L, Zhang, J, Tan, Y, Jiang, Y, Hu, M, Li, M & Zhai, Q, 2014,' Rapid decolorization of anthraquinone and triphenylmethane dye using chloroperoxidase: catalytic mechanism, analysis of products and degradation route', Chemical Engineering journal, Vol, 244, pp. 9–18.
- MJoshi, M, Bansal, R &Purwar, R, 2003, 'Colour removal from textile effluents, Indian J. Fibre & Textile research, Vol. 29, pp. 239–259.
- Forgacs, E, Cserháti, T & Oros, G, 2004, 'Removal of synthetic dyes from wastewaters: a review', Environment International, Vol. 30 no.7, pp. 953–971.
- Manavi, N, Kazemi, AS &Bonakdarpour, B, 2017, 'The development of aerobic granules from conventional activated sludge under anaerobic-aerobic cycles and their adaptation for treatment of dyeing wastewater', Chemical Engineering Journal, Vol. 312, PP.375–384.
- Pan, Y, Wang, Y, Zhou, A, Wang, A, Wu, Z, Lv, L, Li, X, Zhang, K &Zhu,T, 2017, ' Removal of azo dye in an up-flow membrane-less bio electrochemical system integrated with bio-contact oxidation reactor', Chemical Engineering, Vol. 326, pp. 454–461.
- dos Santos, AB, Cervantes, FJ, Lier, JB, 2007, 'Review paper on current technologies for decolourisation of textile wastewaters: perspectives for anaerobic biotechnology', Bioresource Technology, Vol. 98, no. 12, pp. 2369–2385.
- Hashem, FS, Amin, MS, 2016, 'Adsorption of methylene blue by activated carbon derived from various fruit peels', Desalination and Water Treatment, Vol. 57, no. 47, pp. 22573–22584.
- S.M.A. El-Gamal, Amin, MS & Ahmed, MA, 2015, 'Removal of methyl orange and bromophenol blue dyes from aqueous solution using Sorel's cement nanoparticles', Environmental Chemical Engineering, Vol. 3, no. 3 pp. 1702–1712.
- Wang, J, Qin, L, Lin, J, Zhu, J, Zhang, Y, Liu, J & Bruggen, BV, 2017, 'Enzymatic construction of antibacterial ultrathin membranes for dyes removal', Chemical Engineering, Vol. 323, pp. 56–63.
- Hidalgo, A, 2018, 'Behaviour of polysulfone ultrafiltration membrane for dyes removal', Water Science and Technology, Vol.77, no. 8, pp. 2093- 2100.
- Wang, J, Zhang, T, Mei, Y & Pan, B, 2018, 'Treatment of reverse-osmosis concentrate of printing and dyeing wastewater by electro-oxidation process with controlled oxidation-reduction potential (ORP)', Chemosphere, Vol. 201, pp. 621-626.
- Goswami, M & Phukan, P, 2017, 'Enhanced adsorption of cationic dyes using sulfonic acid modified activated carbon', Environmental Chemical Engineering', Vol. 5, no. 4, PP. 3508-3517.
- Manickam, J, 2016, 'Study of water-soluble dyes adsorption from aqueous solution by Prosopis spicigera L. wood (PSLW) carbon', Indian Journal Chemical Technology, Vol. 23, no. 1 pp. 22-30.
- Gaikwad, R & Misal, SA, 2010, 'Applications, Sorption studies of methylene blue on silica gel', International Journal of Chemical Engineering, Vol. 1, no.4, pp. 342-345.
- Zhao, X, Li, M & Lou, X,2013, 'Enhanced photocatalytic activity of zinc oxide synthesized by calcination of zinc sulfide precursor', Material Science in Semiconductor Processing, Vol. 16, no. 2, pp. 489-494.
- Sin, JC, Lam, SM, Lee, KT & Mohamed, AR, 2013, 'Preparation and photocatalytic properties of visible light-driven samarium-doped ZnO nanorods', Ceramics International, Vol. 39, no. 5, pp. 5833-5843.
- Gowthaman, P, Saroja, M. Venkatachalam, M, Deenathayalan, J & Shankar, S, 2014, 'Doping effects of strontium on Zn nonanorods and their photocatalytic properties', Nanoscience and Nano Technology, Vol. 2, no. 4, pp. 377-383.
- Lee, KM, Lai, CW, Ngai, KS & Juan, JC, 2016, 'Recent developments of zinc oxide based photocatalyst in water treatment technology: a review', Water Research, Vol. 88, pp. 428-448.
- Qiao, L,2020, 'Achieving electronic structure reconfiguration in metallic carbides for robust electrochemical water splitting', Materials Chemistry, Vol. 8, no. 5, pp. 2453-2462.
- Nakata, K &Fujishima,A, 2012,'TiO2 photocatalysis: design and applications, Photochemistry Photobiology C Photochemistry Reviews, Vol.13, no. 3, pp. 169-189.
- Ong, CB, Ng, LY & Mohammad, AW, 2018,'A review of ZnO nanoparticles as solar photocatalysts: synthesis, mechanisms and applications', Renewable and Sustainable Energy Reviews, Vol. 81, no. 1, pp. 536-551.
- Szilagyi, IM, 2012, 'WO_3 photocatalysts: influence of structure and composition,' Catalysis, Vol. 294, pp. 119-127.
- Kondo, J,1998, 'Cu2O as a photocatalyst for overall water splitting under visible light irradiation', Chemical Communication, Vol. 3, pp. 357-358.
- Sun, W, Meng, Q, Jing, L, Liu, D, & Cao, Y, 2013, 'Facile synthesis of surface-modified nanosized a-Fe2O3 as efficient visible photocatalysts and mechanism insight', Physical Chemistry C, Vol. 117, no. 3, pp. 1358-1365.
- Malato, S, Fernandez-Ibanez, P, Maldonado, MI, Blanco, J, Gernjak, W, 'Decontamination and disinfection of water by solar photocatalysis: recent overview and trends', Catalysis Today, Vol. 147, no. 1, pp. 1-59.

- Sakthivel, S, Neppolian, B, Shankar, MV, Arabindoo, B, Palanichamy, M & Murugesan, V, 2003, Solar Photocatalytic Degradation of Azo Dye: Comparison of Photocatalytic Efficiency of ZnO and TiO2',Solar Energy Materials and Solar Cells, Vol. 77, no.1, pp. 65–82.
- Sobczynski, A & Dobosz, A, 2001, 'Water purification by photocatalysis on semiconductors', Polish Journal of Environmental Studies, Vol, 10, no. 4, pp. 195–205.
- Wan, Q, Wang, TH & Zhao, JC, 2005, ' Enhanced photocatalytic activity of ZnOnanotetrapods', Applied Physics Letters, Vol. 87, no. 8, pp. 083105-1–083105-3.
- Fox, MA, 1983, 'Organic heterogeneous photocatalysis: chemical conversions sensitized by irradiated semiconductors', Accounts Chemical Research, Vol. 16, no. 9, pp. 314–321.
- Yoneyama, H, Yamashita, Y, & Tamura, H, 1979, 'Heterogeneous photocatalytic reduction of dichromate on n-type semiconductor catalysts', Nature, Vol. 282, no. 5741, pp. 817–818.
- Kogo, K, Yoneyama, H & Tamura,1980, 'Photocatalytic oxidation of cyanide on platinized titanium dioxide', Physical Chemistry, Vol. 84 , no. 13, pp. 1705–1710.
- Pruden, AL & Ollis, DF, 1983,Photoassisted heterogeneous catalysis: The degradation of trichloroethylene in water', Catalysis, Vol. 82, no. 2 pp. 404–417.
- Linsebigler, AL, Lu, G &Yates, JT, 1995, 'Photocatalysis on TiO2 Surfaces: Principles, Mechanisms, and Selected Results', Chemical Reviews, Vol. 95, no. 3, PP. 735–758.
- Herrmann, JM, 1999, 'Heterogeneous photocatalysis: fundamentals and applications to the removal of various types of aqueous pollutants', Catalysis Today, Vol. 53, no. 1, pp. 115–129.
- Gouvea, CA, Wypych, F, Moraes, SG, Duran, N Nagata, N & Peralta-Zamora, P, 2000, 'Semiconductor-assisted photocatalytic degradation of reactive dyes in. aqueous solution', Chemosphere, Vol. 40, no. 4, pp. 433-440.
- Maleki-Ghaleh, M, Shahzadeh, M, Hoseinizadeh, S, Arabi, A, Aghaie, E & Siadati, M, 2016, 'Evaluation of the photo-electro-catalytic behavior of nanostructured ZnO films fabricated by electrodeposition process', Materials Letters, Vol. 169, pp. 140-143.
- Liu, J, Li, X & Dai, L, 2006, 'Water-assisted growth of aligned carbon nanotube-ZnO heterojunction arrays', Advanced Materials, Vol. 18, no. 13, pp. 1740-1744.
- Uskokovic, V & Drofenik, M, 2005, 'Synthesis of materials within reverse micelles', Surface Review Letters, Vol. 12 no. 2, pp. 239-277.
- Kuriakose, S, Satpati, B & Mohapatra, S, 2014, 'Enhanced photocatalytic activity of Co doped ZnOnanodisks and nanorods prepared by a facile wet chemical method', Physical Chemistry Chemical Physics, Vol. 16, no. 25, pp. 12741-12749.
- Achouri, F, 'Porous Mn-doped ZnO nanoparticles for enhanced solar and visible light photocatalysis', Materials Design, Vol. 101, pp. 309-316.
- Yi, S, Cui, J, Li, S, Zhang, L, Wang, D & Lin, Y, 2014, 'Enhanced visible-light photocatalytic activity of Fe/ZnO for rhodamine B degradation and its photogenerated charge transfer properties', Applied Surface Science, Vol. 319, pp. 230-236.
- Meng, A, Xing,J, Li, Z, Li, Q, 2015, 'Cr-doped ZnO nanoparticles: synthesis, characterization, adsorption property, and recyclability', ACS Applied Materials & Interfaces, Vol. 7, no. 49, pp. 27449-27457.
- Mohan, R, Krishnamoorthy, K & Kim, KJ, 2012, 'Enhanced photocatalytic activity of Cu-doped ZnO nanorods', Solid State Communications, Vol. 152, no. 5, pp. 375-380.
- Zhang, X, Chen, Y, Zhang, S & Qiu, C, 2017, 'High photocatalytic performance of high concentration Al-doped ZnO nanoparticles', Separation and Purification Technology, Vol. 172, pp. 236-241.
- Sun, JH, Dong, SY, Feng, JL, Yin, XJ & Zhao, XC, 2011, 'Enhanced sunlight photocatalytic performance of Sn-doped ZnO for Methylene Blue degradation', Molecular Catalysis A: Chemical, Vol. 335, no. 1-2, pp. 145-150.
- Kashif, M, Ali, ME, Syed, M, Usman Ali & Hashim, U, 2013 'Sol–gel synthesis of Pd doped ZnO nanorods for room temperature hydrogen sensing applications', Ceramics International, Vol. 39, no. 6, 6461-6466.
- Alfred B. Anderson & Donald Q. Dowd, 1987, 'CO Adsorption on Pt(ll1) Doped with TiO, FeO, ZnO, and Fe, and Pt Ad-Atoms. Molecular Orbital Study of CO-Dopant Interactions , Physical Chemistry, Vol. 91, no.4, pp. 869-873.
- Bindary, AA, Marsafy, SM, Maddah, AA, 2019, 'Enhancement of the photocatalytic activity of ZnO nanoparticles by silver doping for the degradation of AY99 contaminants', Journal of Molecular Structure, Vol. 1191, pp.76-84.
- Li, D, Nakagawa, Y &Tomishige, K, 2011, 'Methane reforming to synthesis gas over Ni catalysts modified with noble metals, Applied Catalysis: A, Vol. 408, no.1-2, pp. 1– 24.
- Li, B, Kado, S, Mukainakano, Y, Miyazawa, T, Miyao, T, Naito, S, Okumura, K, Kunimori, K &Tomishige, K, 2007, ' Surface modification of Ni catalysts with trace Pt for oxidative steam reforming of methane, Catalysis, Vol. 245, no. 1,pp. 144–155.
- Sattler, JJ, Gonzalez-Jimenez, HB, Luo, ID, Stears, L, Malek, BA, Barton, A, Kilos, DG, Kaminsky, BA, Verhoeven, MP, Koers, GM, Baldus, EJ, Weckhuysen, M &Angew. BA, 2014, 'Platinum-Promoted Ga/Al_2O_3 as Highly Active, Selective, and Stable Catalyst for the Dehydrogenation of Propane', Chemical International Edition, Vol. 53, no. 35, pp. 9251–9256.
- Long, NV, Chien, ND, Hayakawa, T, Hirata, H, Lakshminarayana, G & Nogami, M. 2009, 'The synthesis and characterization of platinum nanoparticles: a method of controlling the size and morphology',Nanotechnology, Vol. 21, no. 3, pp. 035605.
- Xue, XY, Chen, ZH, Chen, YJ, Ma, CH, Xing, LL, Wang, YG & Wang, TH, 2012, 'Abnormal gas sensing characteristics arising from catalyzed morphological changes of ionsorbed oxygen', Nanotechnology, Vol. 21, no. 43, 065501.
- Esfandyarpour, B, Mohajerzadeh, S, Famini, S, Khodadadi, A & Asl Soleimani,2004, 'High sensitivity Pt-doped SnO_2 gas sensors fabricated using sol–gel solution on micromachined (1 0 0) Si substrates, Sensors and Actuators B: chemical, Vol. 100, no. 1-2, pp. 190-194
- Huang, FC, Chen, YY & Wu, TT, 2009, 'A room temperature surface acoustic wave hydrogen sensor with Pt coated ZnO nanorods', Nanotechnology, Vol. 20, no. 6, pp. 065501.
- Tian, LC, Sadik, PW, Norton, DP, Voss, LF, Pearton, SJ, Wang, HT, Kang, BS, Ren, F, Jun, J & Lin, J, 2005, 'Hydrogen sensing at room temperature with Pt-coated ZnO thin films and nanorods, Applied Physics Letters, Vol. 87, no. 22, pp. 222106.
- Gouvea, CA, Wypych, F, Moraes, SG, Duran, N, Nagata, N & Peralta-Zamora, P, 2000, 'Semiconductor-Assisted Photocatalytic Degradation of Reactive Dyes in Aqueous Solution', Chemosphere, Vol. 40, no. 4, pp. 433–440.
- Wu, J & Tseng, CH, 2006 , 'Photocatalytic Properties of nc-Au/ZnO Nanorod Composites', Applied Catalysis :B, Vol. 66, no.1–2, pp. 51–57.
- Wang, X.; Long, H.; Qarony, W.; Tang, C. Y.; Yuan, H.; Tsang, Y. H. Fabrication of luminescent PtS2 quantum dots. J. Lumin. 2019, 211, 227–232.
- 83.Zheng, Y, Zheng, L, Zhan, Y, Lin, X, Zheng, Q & Wei, K, 2007, 'Ag/ZnO Heterostructure Nanocrystals: Synthesis, Characterization, and Photocatalysis', Inorganic Chemistry, Vol. 46, no.17, pp. 6980–6986
- 84. Morales-Flores, U. Pal, N, ESánchez Mor, E, 2011, 'Photocatalytic behavior of ZnO and Pt-incorporated ZnO nanoparticles in phenol degradation', Applied Catalysis A: General, Vol. 394, no. 1-2, PP. 269-275

- 85.Silva, RF, Zaniquelli, M.E.D, 2002,'Morphology of nanometric size particulate aluminium-doped zinc oxide films',Colloids and Surfaces A: Physicochemical and Engineering Aspects, Vol.198-200, pp. 551-558.
- 86. Ahmad, M, Ahmed , E, Ahmed ,W, Elhissi , A, Hongb, ZL, Khalid, NR,2014, 'Enhancing visible light responsive photocatalytic activity by decorating Mn-doped ZnO nanoparticles on graphene', Ceramics international, Vol.40, no. 7, pp. 10085-10097.
- 87. Gurpreet Singh, Sandeep Kumar, Singh, V.P. & Rahul Vaish, 2019, 'Transparent ZnO crystallized glass ceramics for photocatalytic and antibacterial applications', Applied. Physics, Vol. 125, pp. 175102-175111.